Nanoscale

COMMUNICATION

View Article Online
View Journal | View Issue

Cite this: *Nanoscale*, 2018, **10**, 15436

Received 16th June 2018,
Accepted 25th July 2018

DOI: 10.1039/c8nr04895a

rsc.li/nanoscale

In situ synthesis and macroscale alignment of $CsPbBr_3$ perovskite nanorods in a polymer matrix†

Juan He, ‡[a] Andrew Towers,‡[b,c] Yanan Wang,§‡[b] Peisen Yuan, [d] Zhang Jiang,[e] Jiangshan Chen,[d] Andre J. Gesquiere,*[a,b,c,f] Shin-Tson Wu *[a] and Yajie Dong *[a,b,f]

We report an *in situ* catalyst-free strategy to synthesize inorganic $CsPbBr_3$ perovskite nanorods in a polymer matrix (NRs-PM) with good dimensional control, outstanding optical properties and ultrahigh environmental stability. Polarization photoluminescence (PL) imaging with high spatial resolution was carried out for the first time on single nanorod (NR) and shows a relatively high local polarization ratio (~0.4) consistent with theoretical predictions based on a dielectric contrast model. We further demonstrate that macroscale alignment of the $CsPbBr_3$ nanorods can be achieved through mechanically stretching the NRs-PM films at elevated temperature, without deteriorating the optical quality of the NRs. A polarization ratio of 0.23 is observed for these aligned NRs-PM films, suggesting their potential as polarized down-converters to increase the light efficiency in liquid crystal display (LCD) backlights.

One dimensional (1D) semiconductor nanowires (NWs)[1–5] or nanorods (NRs)[6,7] have long been considered as fundamental building blocks in nanoscience and technologies. Macroscale alignment of these building blocks could lead to functional structures or devices for electronics,[2,8] photonics,[3] or optoelectronics[4,9,10] applications. Aligned cadmium selenide (CdSe) based nanorods have been suggested for polarized light sources[11–18] which are of particular interest in liquid crystal display (LCD) back lighting[19–21] for enhanced optical efficiency. However, their relatively complicated synthetic process, high production cost and challenge with regard to macroscale alignment have limited their adoption in the display industry.[22,23] A low cost, easy-to-align 1D luminescent nanomaterial system with polarized emission is thus highly desired.

Metal halide perovskites with a general formula of ABX_3, where A is methylammonium (MA), formamidinium (FA) or Cs, B is Pb or Sn, and X is Cl, Br, or I, have been under active investigation recently as promising low cost, high performance photovoltaic or light emitting materials.[24–33] Among them, purely inorganic $CsPbX_3$ have been of special interest for their intrinsically higher stability compared to their organic–inorganic hybrid counterparts.[33–36] Specifically, $CsPbBr_3$ has shown high emission efficiency and outstanding color purity,[33,36,37] and 1D $CsPbBr_3$ nanostructures have demonstrated polarized emission.[38–40] Various synthetic methods have been investigated to achieve perovskite NWs/NRs, either in the solution-phase[41–50] or in the vapor phase[51] with considerable size and shape control and sometimes local alignment.[38] However, macroscale alignment of $CsPbBr_3$ perovskite NWs/NRs remains challenging. This is mainly because even with all-inorganic nanostructures, $CsPbX_3$ are still susceptible to heat and moisture.[38] Moreover, NWs in close contact tend to aggregate and re-grow into bulk structures.[48]

Here we report an *in situ* catalyst-free strategy to synthesize $CsPbBr_3$ nanorods in a polymer matrix (NRs-PM) with high stability that enables macroscale alignment without luminescence degradation.

The synthesis takes advantage of a simple swelling–deswelling microencapsulation (SDM) strategy recently demonstrated by our group.[52] As schematically shown in Fig. 1a, the $CsPbBr_3$ perovskite precursor solution was introduced into a polymer matrix (*e.g.* polystyrene) through a solvent-induced swelling process and distributed in-between the swollen polymer chains as stripe-shaped droplets. Subsequently, in an anneal-

[a]*College of Optics and Photonics, University of Central Florida, Orlando, Florida, USA. E-mail: yajie.dong@ucf.edu, swu@creol.ucf.edu, andre@ucf.edu*
[b]*NanoScience Technology Center, University of Central Florida, Orlando, Florida, USA*
[c]*Department of Chemistry, University of Central Florida, Orlando, Florida, USA*
[d]*Institute of Polymer Optoelectronic Materials and Devices, State Key Laboratory of Luminescent Materials and Devices, South China University of Technology, Guangzhou, China*
[e]*X-ray Science Division, Advanced Photon Source, Argonne National Laboratory, Argonne, Illinois, USA*
[f]*Department of Materials Science & Engineering, University of Central Florida, Orlando, Florida, USA*

†Electronic supplementary information (ESI) available. See DOI: 10.1039/c8nr04895a

‡These authors contributed equally.

§Present address: Laboratory of Advanced Optoelectronic Materials, College of Chemistry, Chemical Engineering and Materials Science, Soochow University, Suzhou 215123, China.

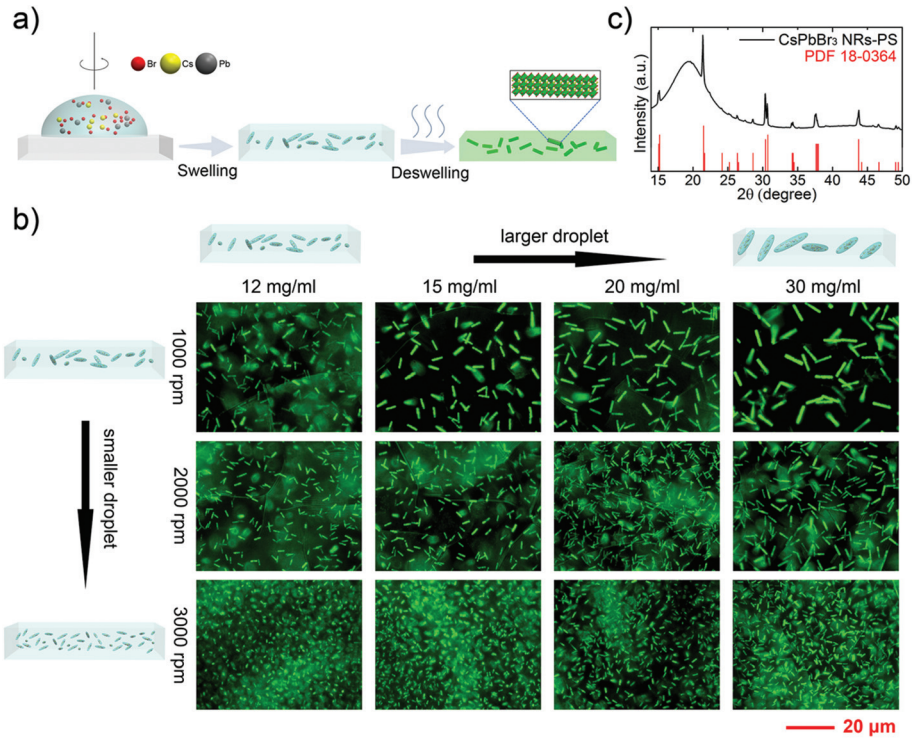

Fig. 1 *In situ* synthesis of luminescent $CsPbBr_3$ NRs-PM. (a) Scheme of the $CsPbBr_3$ NRs-PM formation process through SDM. (b) Fluorescence microscopy images of NRs-PM synthesized with different precursor concentrations and different spin-coating speeds. Focal planes were adjusted to be ~4–5 mm underneath the top surface for all samples. The insets on the top and left are schematic illustrations for the droplet size under different conditions. (c) XRD pattern of $CsPbBr_3$ NRs-PS with standard monoclinic $CsPbBr_3$ (PDF 18-0364) as a reference.

ing process, the solvent was driven out of the polymer matrix and perovskite nanocrystal nucleation began soon after the solvent evaporated. This allowed precursors in droplets to reach supersaturation, which was followed by perovskite nanorod growth within the confinement of the surrounding polymer chain clusters. Meanwhile, the polymer matrix deswelled and shrank, passivating and protecting the perovskite nanorods (see the ESI† for Experimental details).

In this system, the precursor content in each droplet has a direct effect on $CsPbBr_3$ NRs' size. It is therefore important to carefully monitor the applied precursor concentration to achieve the control of NR size. Considering the kinetics of precursor distribution in the polymer matrix, a lower precursor concentration leads to a lower solution viscosity, which facilitates the formation of smaller droplets during the SDM process, thus generating smaller NRs. Increasing the rotational speed of the spin-coating process leads to more vigorous distribution of precursor droplets, also resulting in a smaller droplet size and thus smaller NRs.

Inspection of NRs in a polystyrene matrix (NRs-PS) prepared with different precursor concentrations or spin-coating speeds by fluorescence microscopy (Fig. 1b) clearly shows that the NR size can be reduced either by lowering the precursor concentration or by increasing the spin speed. The length of NRs can be tuned from as short as 1.27 ± 0.16 μm obtained with 12 mg ml^{-1} $CsPbBr_3$ precursor at a speed of 3000 rpm to as long as 7.15 ± 0.43 μm with 30 mg ml^{-1} precursor at 1000 rpm speed (Fig. S1†), with a standard deviation no more than 12% and actually less than 9% under most of the conditions (Fig. S2†). The aspect ratios of the NRs synthesized at 1000 rpm/2000 rpm spin speed can be derived from the fluorescence microscopy images, with values ranging from 7.66 to 10.88 (Fig. S3†). It is also worth noting that these NRs are only observed with the microscope focal plane tuned to be several micrometers underneath the top surface, indicating good encapsulation with deswelled polymers.

XRD characterization was carried out to identify the crystal structure of the NRs-PM (Fig. 1c). Although overlapped with the broad band polystyrene signal, clear sharp peaks from $CsPbBr_3$ NRs can be recognized, which match very well with the monoclinic structure of $CsPbBr_3$ (standard PDF card 18-0364). Lattice constants a and c were determined to be 5.84 Å and 5.88 Å, respectively.

Our *in situ* SDM strategy is not limited to polystyrene substrates and appears to be a feasible synthesis strategy for most polymers that undergo a swelling–deswelling process when interacting with DMF solvent. In fact, fluorescent NRs-PMs were also obtained with other polymer substrates such as polycarbonate (PC) or acrylonitrile butadiene styrene (ABS) (Fig. S4†). The rod sizes are not identical for different polymers even when the same precursors and processing procedures were used. This is not surprising since the intrinsic polymer pro-

perties, such as the swelling ratio in DMF solvent, polymer chain length, cluster morphology, *etc.*, can vary for different polymers and may have a key impact on the dynamics of droplet distribution.

Fig. 2a shows the absorption and photoluminescence (PL) spectra of typical NRs-PS samples, with the absorption exciton peak at 520 nm and the emission peak at around 526 nm. NRs-PS prepared under different conditions share the same exciton peak wavelength and only show different optical densities with precursors of different concentrations (Fig. S5†). This result indicates that the rod size does not influence the optical properties too much, mainly because the NRs are in the μm or sub-μm scale and the quantum confinement effect doesn't play an important role. Similarly, the PL emission peak is only slightly shifted within the 2–3 nm range for samples under different processing conditions, as shown in Table S1.† The narrow 18 nm full width at half maximum (FWHM) of the emission peak indicates excellent crystallinity and the lack of defect states. Time-resolved PL decay of the NRs shows an average radiative lifetime τ_{avg} of ~50 ns, which is shorter than that observed for $MAPbBr_3$-PS (130 ns),[52] as similarly noticed in ref. 33. The NRs-PS films prepared under different conditions have photoluminescence quantum yield (PLQY) values ranging from 23% to 30% (Table S2†).

For NRs, it is of great interest to see if their emission has some special properties with respect to their anisotropic shape. We therefore acquired single particle polarization PL images of the NRs-PS using a home-built sample-scanning confocal microscope (Fig. S6†).

The sample was imaged over a 15 × 15 μm^2 area including two NRs. The intensities of two perpendicular polarized PL signals (I_x and I_y) were collected simultaneously (Fig. S7†). The resulting polarization P ($P = (I_y - I_x)/(I_y + I_x)$) image is shown in Fig. 2c. The upper right rod which lies parallel to the y axis mostly shows positive P values, as illustrated in the upper histogram in Fig. 2d, indicating that the PL emission is mostly polarized along the rod axis ($I_x < I_y$). On the other hand, the rod lying in the nearly perpendicular direction in the lower left corner is mapped with more negative P value points (Fig. 2d, lower histogram), corresponding to $I_x > I_y$. This indicates that NRs with perpendicular orientations tend to cancel the PL polarization of each other, and thus macroscale NR alignment is necessary to avoid this polarization cancellation effect.

The origin of polarized emission of the $CsPbBr_3$ NRs-PS can be attributed to the dielectric contrast between the NRs and the surrounding polymer matrix environment.[53] With the dielectric constants of $CsPbBr_3$ (6.35) and surrounding PS (2.6), the theoretical P of an infinitely long 1D nanostructure is calculated to be ~0.47 (ESI†). For NRs with a limited aspect ratio, it is reasonable to see that most of the P values are lower than this limit. The P value of single NRs could be further enhanced by increasing NRs' aspect ratio or using a polymer matrix with an even lower dielectric constant.

The intimate passivation of the perovskite NRs by the surrounding polymer matrix yields great environmental stability even without further encapsulation. One as-obtained NRs-PS sheet with an initial PLQY of 29% was cut into two pieces and placed in air and water respectively, with their luminescence periodically monitored. Interestingly, the NRs-PS became much brighter after being immersed in water for 277 days (Fig. 3a). In fact, the PLQY increased to 40% within two weeks and then remained steady (Fig. S8†). The piece stored in air ended up with a PLQY of 31%.

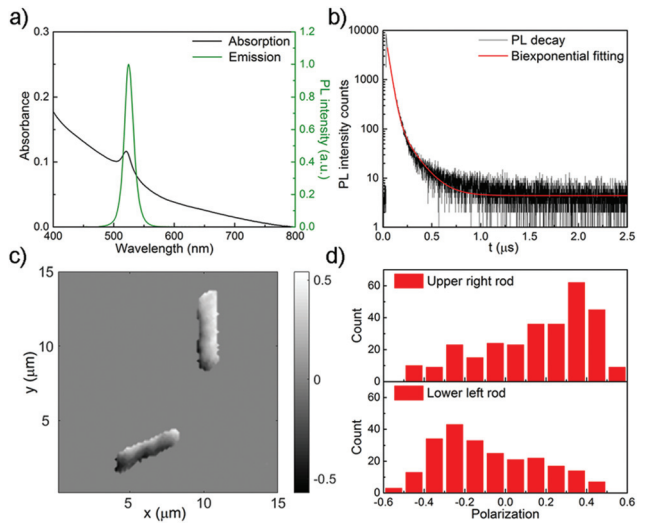

Fig. 2 Optical properties of $CsPbBr_3$ NRs-PS. (a) UV-Vis absorption and PL spectra of NRs-PS (15 mg ml^{-1} precursor, 2000 rpm). (b) PL decay (black) and the corresponding fit (red) of NRs-PS. (c) Polarization map of NRs-PS. (d) Histograms of P (polarization) values obtained from the upper right rod (up) and lower left rod (down) in (c).

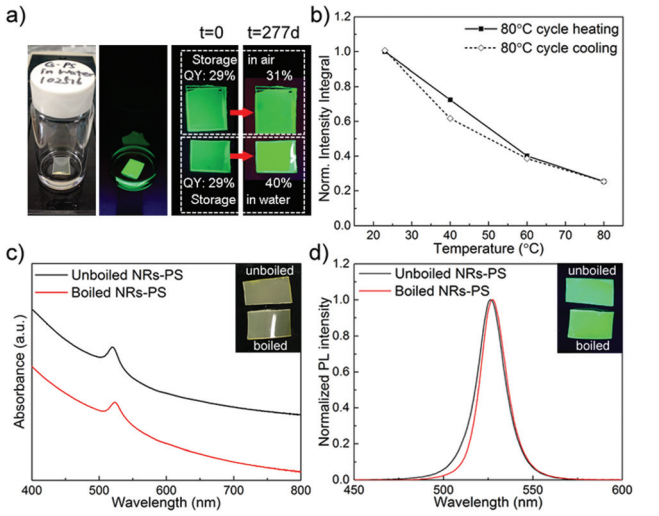

Fig. 3 Water and thermal stability characterization. (a) Photographs of the $CsPbBr_3$ NRs-PS film immersed in water. From left to right: the NRs-PS film stored in a water bottle under ambient or UV illumination; film brightness and PLQY at the beginning and after 277 days (the top piece stored in air and the bottom piece stored in water). (b) Temperature dependent PL of NRs-PS, (c) absorption and (d) PL emission spectra of the $CsPbBr_3$ NRs-PS film before (black) and after (red) boiling treatment.

Moisture enhanced PL in perovskite films has been reported before.[54–59] The temporal PL enhancement was often attributed to reversible hydration and self-healing of the perovskite lattice by hydrogen bonding induced deactivation of nonradiative recombination centers.[60–64] Such an enhancement is usually observed in a relatively short period and further moisture exposure dissolves the perovskite materials and eventually leads to material decomposition and luminescence decay.[65] Here, with the intimate protection of the polymer matrix, a very limited amount of water molecules can penetrate inside to assist in the perovskite self-healing process over an extended period, yet they don't appear to be able to induce perovskite dissolution. The absorption and PL spectra before and after the extended water immersion test did not change much except that the PL spectrum becomes slightly narrower (with the FWHM decreased for 1 nm) after water storage (Fig. S9†), which is attributed to the healing of defects in the NRs and further confirms their outstanding long-term stability.

Thermal stability was evaluated by heating up the NRs-PS film to 80 °C, which is close to PS's glass transition temperature, and then cooling back to room temperature (RT). The NR emission was quenched at higher temperature but could be fully recovered back at RT, as shown in Fig. 3b. The absorption and PL emission spectra are identical before and after the heating process (Fig. S10†). To further test the performance under harsh treatment, half of the NRs-PS film was cut and put into boiling water (ESI Video†) for 30 seconds. Even though the boiled piece curved due to high temperature (Fig. 3c inset), the boiled and unboiled samples showed similar luminescent brightness under UV illumination (Fig. 3d inset). The absorption of the film remained unchanged after boiling (Fig. 3c), while the PL spectrum narrowed (Fig. 3d). As discussed above, heating treatment alone wouldn't induce such an effect, so it is likely due to the water-assisted healing effect similar to that observed in the water-immersed sample but now accelerated by the higher temperature.

The water induced PL enhancement and healing effect was also observed for the boiled NRs-PC sample and the NRs-ABS sample stored in water for more than four months (the NRs-ABS sample was not boiled because the glass transition temperature of ABS is lower than 100 °C), as shown in Fig. S11–14.† This indicates that the NRs-PM synthesized with our SDM strategy can generally benefit from such a healing effect to obtain better optical performance.

To utilize the above demonstrated polarized PL of the NRs and avoid the cancellation effect caused by random orientation distribution, macroscale alignment of these NRs is critical. The outstanding stability of the NRs-PM makes this feasible through simple mechanical stretching at elevated temperature. PS has a moderate glass transition temperature which allowed lab-testing of this concept. Being heated with a heat gun in air (Fig. 4a), the NRs-PS film was steadily stretched to a final length that was 8 times longer. Well aligned NRs were found with 37% of them lying in the ±1.5° range and 80% lying in the ±4.5° range (Fig. 4b) with respect to the stretching direction. The angle dependent PL intensity for NRs-PS samples

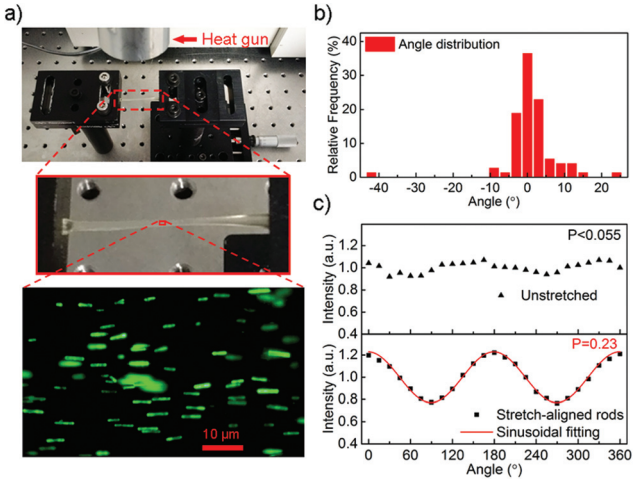

Fig. 4 Stretch-alignment of $CsPbBr_3$ NRs-PS. (a) Top: setup for stretching the NRs-PS film; middle: enlarged NRs-PS sample illustration; bottom: fluorescence microscopy image of stretch-aligned NRs. (b) Angle distribution of stretch-aligned NRs (bottom image of (a)). The elongation ratio is 8 to 1. (c) PL polarization of unstretched (top)/stretch-aligned (bottom) NRs-PS.

was measured using the setup shown in Fig. S15† and polarization P_s was derived from $P_s = (I_{max} - I_{min})/(I_{max} + I_{min})$ (Fig. 4c). The minor polarization of the NRs-PS film before stretching was attributed to the uneven distribution of NR orientations. The PL angular dependence of the stretch-aligned NRs-PS complies well with a sinusoidal shape, with the maximum along the rod axis and the obtained highest P_s around 0.23. The polarization levels of stretch-aligned NRs-PS synthesized under different conditions are listed in Table S3,† which are positively correlated with the aspect ratios of these NRs (Fig. S16†). As an average effect of polarized emission from all NRs, the polarization levels of these macroscale samples are consistent with the P value statistics obtained in single NR polarization PL imaging. Moreover, the polarized PL is almost independent of the polarization of the excitation laser beam (Fig. S17†).

We believe that the process of stretching and aligning the NRs-PM film can easily be carried out on a large scale given the maturity of industrial polymer processing techniques. With a polarization value of 0.23, the aligned NRs-PM film can possibly improve the transmitted backlight in liquid crystal displays (LCD) from 50% to 62%.[66] Furthermore, the polarization level of aligned NRs can be improved by obtaining a larger NR aspect ratio and using a lower dielectric constant polymer material as the matrix.

Conclusions

In summary, we demonstrated a simple and general strategy to achieve *in situ* synthesis of stable, luminescent $CsPbBr_3$ perovskite NRs-PM with excellent emission color purity and size control. Polarized emission from single NR along the long

axis was observed in polarized PL imaging. Without further encapsulation, NRs-PM demonstrated excellent water and thermal stabilities and can survive harsh treatment with retained or even enhanced luminescence efficiency. The NRs-PM can be easily aligned with good direction uniformity on the macroscale and show polarized emission with a polarization value of 0.23. With further investigations and improvements in emission polarization, the perovskite NRs-PM could be promising building blocks for more efficient LCD backlight or other optical and photonic applications.

Conflicts of interest

There are no conflicts to declare.

Acknowledgements

Y. Dong is grateful for support of this work by the University of Central Florida through a startup funding (Grant No. 20080738). This research used resources of the Advanced Photon Source, a U.S. Department of Energy (DOE) Office of Science User Facility operated for the DOE Office of Science by Argonne National Laboratory under Contract No. DE-AC02-06CH11357. The authors thank Dr Martin Schadt and Dr Le Zhou for helpful discussion.

Notes and references

1 A. Zhang, G. Zheng and C. M. Lieber, *Nanowires: Building Blocks for Nanoscience and Nanotechnology*, Springer, New York, 2016.
2 W. Lu and C. M. Lieber, *Nat. Mater.*, 2007, **6**, 841.
3 R. Yan, D. Gargas and P. Yang, *Nat. Photonics*, 2009, **3**, 569.
4 Y. Li, F. Qian, J. Xiang and C. M. Lieber, *Mater. Today*, 2006, **9**, 18.
5 P. Yang, R. Yan and M. Fardy, *Nano Lett.*, 2010, **10**, 1529.
6 A. P. Alivisatos, *Science*, 1996, **271**, 933.
7 X. Peng, L. Manna, W. Yang, J. Wickham, E. Scher, A. Kadavanich and A. P. Alivisatos, *Nature*, 2000, **404**, 59.
8 Y. Cui and C. M. Lieber, *Science*, 2001, **291**, 851.
9 X. Duan, Y. Huang, Y. Cui, J. Wang and C. M. Lieber, *Nature*, 2001, **409**, 66.
10 W. U. Huynh, J. J. Dittmer and A. P. Alivisatos, *Science*, 2002, **295**, 2425.
11 J. Hu, L. S. Li, W. Yang, L. Manna, L. W. Wang and A. P. Alivisatos, *Science*, 2001, **292**, 2060.
12 C. X. Shan, Z. Liu and S. K. Hark, *Phys. Rev. B: Condens. Matter Mater. Phys.*, 2006, **74**, 8.
13 I. Hadar, G. B. Hitin, A. Sitt, A. Faust and U. Banin, *J. Phys. Chem. Lett.*, 2013, **4**, 502.
14 A. Sitt, A. Salant, G. Menagen and U. Banin, *Nano Lett.*, 2011, **11**, 2054.
15 D. V. Talapin, R. Koeppe, S. Götzinger, A. Kornowski, J. M. Lupton, A. L. Rogach, O. Benson, J. Feldmann and H. Weller, *Nano Lett.*, 2003, **3**, 1677.
16 I. Hadar, J. P. Philbin, Y. E. Panfil, S. Neyshtadt, I. Lieberman, H. Eshet, S. Lazar, E. Rabani and U. Banin, *Nano Lett.*, 2017, **17**, 2524.
17 G. Yang, H. Zhong, Z. Bai, R. Liu and B. Zou, *Adv. Opt. Mater.*, 2014, **2**, 885.
18 Y. Gao, V. D. Ta, X. Zhao, Y. Wang, R. Chen, E. Mutlugun, K. E. Fong, S. T. Tan, C. Dang, X. W. Sun, H. Sun and H. V. Demir, *Nanoscale*, 2015, **7**, 6481.
19 A. K. Srivastava, W. Zhang, J. Schneider, A. L. Rogach, V. G. Chigrinov and H. S. Kwok, *Adv. Mater.*, 2017, **29**, 1701091.
20 K. Neyts, M. Mohammadimasoudi, Z. Hens and J. Beeckman, *SID Symp. Dig. Tech. Papers*, 2016, **47**, 552.
21 P. D. Cunningham, J. B. Souza Jr., I. Fedin, C. She, B. Lee and D. V. Talapin, *ACS Nano*, 2016, **10**, 5769.
22 M. Hasegawa, Y. Hirayama and S. Dertinger, *SID Symp. Dig. Tech. Papers*, 2015, **46**, 67.
23 M. Hasegawa and Y. Hirayama, *SID Symp. Dig. Tech. Papers*, 2016, **47**, 241.
24 D. Bi, W. Tress, M. I. Dar, P. Gao, J. Luo, C. Renevier, K. Schenk, A. Abate, F. Giordano, J. P. C. Baena and J. D. Decoppet, *Sci. Adv.*, 2016, **2**, e1501170.
25 B. Luo, Y. C. Pu, S. A. Lindley, Y. Yang, L. Lu, Y. Li, X. Li and J. Z. Zhang, *Angew. Chem., Int. Ed.*, 2016, **55**, 8864.
26 H. Cho, S. H. Jeong, M. H. Park, Y. H. Kim, C. Wolf, C. L. Lee, J. H. Heo, A. Sadhanala, N. Myoung, S. Yoo and S. H. Im, *Science*, 2015, **350**, 1222.
27 S. D. Stranks and H. J. Snaith, *Nat. Nanotechnol.*, 2015, **10**, 391.
28 L. Zhang, X. Yang, Q. Jiang, P. Wang, Z. Yin, X. Zhang, H. Tan, Y. M. Yang, M. Wei, B. R. Sutherland and E. H. Sargent, *Nat. Commun.*, 2017, **8**, 15640.
29 S. A. Veldhuis, P. P. Boix, N. Yantara, M. Li, T. C. Sum, N. Mathews and S. G. Mhaisalkar, *Adv. Mater.*, 2016, **28**, 6804.
30 M. A. Green, A. Ho-Baillie and H. J. Snaith, *Nat. Photonics*, 2014, **8**, 506.
31 X. He, Y. Qiu and S. Yang, *Adv. Mater.*, 2017, **29**, 1700775.
32 Q. Zhou, Z. Bai, W. G. Lu, Y. Wang, B. Zou and H. Zhong, *Adv. Mater.*, 2016, **28**, 9163.
33 L. Protesescu, S. Yakunin, M. I. Bodnarchuk, F. Krieg, R. Caputo, C. H. Hendon, R. X. Yang, A. Walsh and M. V. Kovalenko, *Nano Lett.*, 2015, **15**, 3692.
34 Y. Wang, X. Li, J. Song, L. Xiao, H. Zeng and H. Sun, *Adv. Mater.*, 2015, **27**, 7101.
35 M. Kulbak, D. Cahen and G. Hodes, *J. Phys. Chem. Lett.*, 2015, **6**, 2452.
36 A. Swarnkar, R. Chulliyil, V. K. Ravi, M. Irfanullah, A. Chowdhury and A. Nag, *Angew. Chem., Int. Ed.*, 2015, **127**, 15644.
37 X. Li, Y. Wu, S. Zhang, B. Cai, Y. Gu, J. Song and H. Zeng, *Adv. Funct. Mater.*, 2016, **231**, 2435.

38 S. N. Raja, Y. Bekenstein, M. A. Koc, S. Fischer, D. Zhang, L. Lin, R. O. Ritchie, P. Yang and A. P. Alivisatos, *ACS Appl. Mater. Interfaces*, 2016, **8**, 35523.
39 W. G. Lu, X. G. Wu, S. Huang, L. Wang, Q. Zhou, B. Zou, H. Zhong and Y. Wang, *Adv. Opt. Mater.*, 2017, **5**, 1700594.
40 D. Wang, D. Wu, D. Dong, W. Chen, J. Hao, J. Qin, B. Xu, K. Wang and X. Sun, *Nanoscale*, 2016, **8**, 11565.
41 Y. Fu, H. Zhu, C. C. Stoumpos, Q. Ding, J. Wang, M. G. Kanatzidis, X. Zhu and S. Jin, *ACS Nano*, 2016, **10**, 7963.
42 H. Zhu, Y. Fu, F. Meng, X. Wu, Z. Gong, Q. Ding, M. V. Gustafsson, M. T. Trinh, S. Jin and X. Y. Zhu, *Nat. Mater.*, 2015, **14**, 636.
43 S. W. Eaton, M. Lai, N. A. Gibson, A. B. Wong, L. Dou, J. Ma, L. W. Wang, S. R. Leone and P. Yang, *Proc. Natl. Acad. Sci. U. S. A.*, 2016, **113**, 1993.
44 P. Zhu, S. Gu, X. Shen, N. Xu, Y. Tan, S. Zhuang, Y. Deng, Z. Lu, Z. Wang and J. Zhu, *Nano Lett.*, 2016, **16**, 871.
45 H. Deng, D. Dong, K. Qiao, L. Bu, B. Li, D. Yang, H. E. Wang, Y. Cheng, Z. Zhao, J. Tang and H. Song, *Nanoscale*, 2015, **7**, 4163.
46 A. B. Wong, M. Lai, S. W. Eaton, Y. Yu, E. Lin, L. Dou, A. Fu and P. Yang, *Nano Lett.*, 2015, **15**, 5519.
47 D. Zhang, S. W. Eaton, Y. Yu, L. Dou and P. Yang, *J. Am. Chem. Soc.*, 2015, **137**, 9230.
48 M. J. Ashley, M. N. O'Brien, K. R. Hedderick, J. A. Mason, M. B. Ross and C. A. Mirkin, *J. Am. Chem. Soc.*, 2016, **138**, 10096.
49 S. Sun, D. Yuan, Y. Xu, A. Wang and Z. Deng, *ACS Nano*, 2016, **10**, 3648.
50 L. Dou, M. Lai, C. S. Kley, Y. Yang, C. G. Bischak, D. Zhang, S. W. Eaton, N. S. Ginsberg and P. Yang, *Proc. Natl. Acad. Sci. U. S. A.*, 2017, **114**, 7216.
51 J. Xing, X. F. Liu, Q. Zhang, S. T. Ha, Y. W. Yuan, C. Shen, T. C. Sum and Q. Xiong, *Nano Lett.*, 2015, **15**, 4571.
52 Y. Wang, J. He, H. Chen, J. Chen, R. Zhu, P. Ma, A. Towers, Y. Lin, A. J. Gesquiere, S. T. Wu and Y. Dong, *Adv. Mater.*, 2016, **28**, 10710.
53 J. Wang, M. S. Gudiksen, X. Duan, Y. Cui and C. M. Lieber, *Science*, 2001, **293**, 1455.
54 G. E. Eperon, S. N. Habisreutinger, T. Leijtens, B. J. Bruijnaers, J. J. van Franeker, D. W. deQuilettes, S. Pathak, R. J. Sutton, G. Grancini, D. S. Ginger, R. A. Janssen, A. Petrozza and H. J. Snaith, *ACS Nano*, 2015, **9**, 9380.
55 W. Zhou, Y. Zhao, C. Shi, H. Huang, J. Wei, R. Fu, K. Liu, D. Yu and Q. Zhao, *J. Phys. Chem. C*, 2016, **120**, 4759.
56 X. Gong, M. Li, X. B. Shi, H. Ma, Z. K. Wang and L. S. Liao, *Adv. Funct. Mater.*, 2015, **25**, 6671.
57 J. You, Y. Yang, Z. Hong, T. B. Song, L. Meng, Y. Liu, C. Jiang, H. Zhou, W. H. Chang, G. Li and Y. Yang, *Appl. Phys. Lett.*, 2014, **105**, 183902.
58 Z. Zhu, V. G. Hadjiev, Y. Rong, R. Guo, B. Cao, Z. Tang, F. Qin, Y. Li, Y. Wang, F. Hao and S. Venkatesan, *Chem. Mater.*, 2016, **28**, 7385.
59 S. G. R. Bade, J. Li, X. Shan, Y. Ling, Y. Tian, T. Dilbeck, T. Besara, T. Geske, H. Gao, B. Ma and K. Hanson, *ACS Nano*, 2016, **10**, 1795.
60 X. Zhang, X. Bai, H. Wu, X. Zhang, C. Sun, Y. Zhang, W. Zhang, W. Zheng, W. W. Yu and A. L. Rogach, *Angew. Chem., Int. Ed.*, 2018, **57**, 3337.
61 K. K. Bass, R. E. McAnally, S. Zhou, P. I. Djurovich, M. E. Thompson and B. C. Melot, *Chem. Commun.*, 2014, **50**, 15819.
62 C.-H. Chiang, M. K. Nazeeruddin, M. Gratzel and C.-G. Wu, *Energy Environ. Sci.*, 2017, **10**, 808.
63 R. L. Z. Hoye, M. R. Chua, K. P. Musselman, G. Li, M.-L. Lai, Z.-K. Tan, N. C. Greenham, J. L. MacManus-Driscoll, R. H. Friend and D. Credgington, *Adv. Mater.*, 2015, **27**, 1414.
64 A. M. Leguy, Y. Hu, M. Campoy-Quiles, M. I. Alonso, O. J. Weber, P. Azarhoosh, M. Van Schilfgaarde, M. T. Weller, T. Bein, J. Nelson and P. Docampo, *Chem. Mater.*, 2015, **27**, 3397.
65 J. M. Frost, K. T. Butler, F. Brivio, C. H. Hendon, M. Van Schilfgaarde and A. Walsh, *Nano Lett.*, 2014, **14**, 2584.
66 J. He, Y. Wang, H. Chen, A. Towers, P. Yuan, Z. Jiang, C. Zhang, J. Chen, A. J. Gesquiere, S. T. Wu and Y. Dong, *SID Symp. Dig. Tech. Papers*, 2018, **49**, 218.